Journal of Materials Chemistry B

ROYAL SOCIETY OF CHEMISTRY

PAPER

View Article Online
View Journal

Cite this: DOI: 10.1039/d5tb02774h

Engineering functionalized carbon dots as biocompatible nanocarriers for controlled doxorubicin delivery in cancer therapy

Sandra Rodríguez-Varillas,[a] Tania Fontanil,[b] Jorge Espina-Casado,[c] Alfonso Fernández-González,[a] Rosana Badía-Laíño *[a] and Santiago Cal[d]

Cancer remains one of the leading causes of mortality worldwide, emphasizing the urgent need for therapeutic strategies that are both effective and biocompatible. Advances in nanotechnology have enabled the development of innovative drug delivery systems with improved pharmacological profiles. Among these, carbon dots (CDs) have emerged as versatile nanomaterials owing to their intrinsic luminescence, facile synthesis, excellent biocompatibility, and antioxidant activity. Their surface modification with cyclodextrins (Cyds) further enhances functionality by enabling host–guest complexation with therapeutic molecules. In this work, we designed and comparatively evaluated β- and γ-cyclodextrin-functionalized carbon dots (β-Cyd-CDs and γ-Cyd-CDs) as nanocarriers for the anthracycline drug doxorubicin (DOX), with the aim of elucidating how cyclodextrin cavity size influences drug–carrier interactions and release behavior. Spectroscopic analyses confirmed DOX binding through inclusion complex formation, leveraging the luminescent behavior of CDs to monitor interaction events. Drug loading studies revealed that β-Cyd-CD exhibited significantly higher loading efficiency than γ-Cyd-CD, highlighting the influence of cyclodextrin cavity size on host–guest complexation with doxorubicin. Drug release experiments under physiological-like conditions revealed a moderated and sustained release profile, with release rates approximately 25–60% slower than free DOX, attributed to the combined effects of cyclodextrin inclusion and surface interactions within the nanoplatform. *In vitro* assays demonstrated that DOX-loaded Cyd-CDs retained potent antiproliferative activity against tumor cells while exhibiting reduced cytotoxicity toward normal fibroblasts. These findings demonstrate that cyclodextrin-functionalized carbon dots constitute a versatile supramolecular nanoplatform for controlled drug delivery, where host–guest interactions can be rationally tuned to modulate drug loading and release behavior.

Received 11th December 2025,
Accepted 8th April 2026

DOI: 10.1039/d5tb02774h

rsc.li/materials-b

Introduction

Cancer remains a major global health concern due to its high mortality rates, highlighting the urgent need for novel, effective, and safe therapeutic strategies.[1] This pathology is characterized by the uncontrolled proliferation of malignant cells, which invade surrounding tissues and disrupt the normal biological functions of healthy cells, posing a significant health risk to affected individuals.[2] Although cancer therapy has advanced significantly over the last decades thanks to approaches such as phototherapy, gene therapy, hormone therapy, and immunotherapy, the most commonly employed treatments continue to be surgery, radiotherapy and chemotherapy,[3] with the latter remaining one of the most effective options currently available. Doxorubicin (marketed as Adriamycin®) is a widely used antineoplastic agent for the treatment of both hematologic and solid tumors,[4] including breast and bladder cancer, leukemia, and sarcoma.[5]As illustrated in Fig. 1, its mechanism of action involves intercalation between DNA base pairs, distortion of the helical structure, inhibition of topoisomerase-II activity, and the generation of reactive oxygen species, ultimately leading to suppression of cell proliferation and the induction of apoptosis.[4,5]

Despite its potent antitumor activity, characterized by high cellular uptake and cytotoxicity, the use of doxorubicin is related to severe side effects including hepatotoxicity, cardiotoxicity, myelosuppression, nephrotoxicity, and multidrug resistance.[5]

[a] Department of Physical and Analytical Chemistry, University of Oviedo, Spain. E-mail: rbadia@uniovi.es
[b] Department of Functional Biology, University of Oviedo, Spain
[c] Scientific-Technical Services, University of Oviedo, Spain
[d] Department of Biochemistry and Molecular Biology, Faculty of Medicine, University of Oviedo, Spain

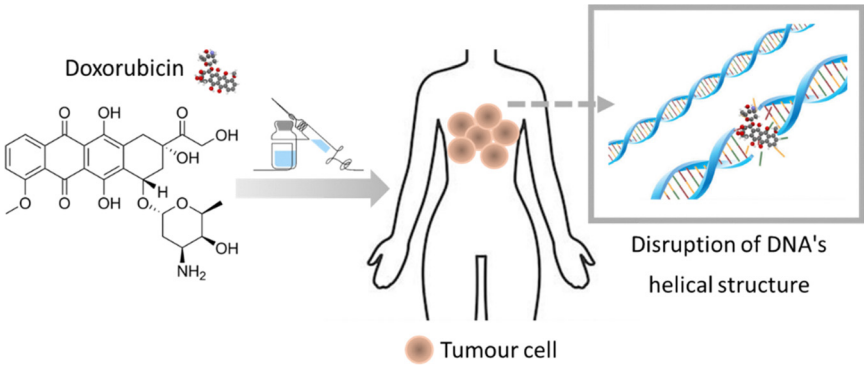

Fig. 1 Mechanism of action of the chemotherapeutic agent doxorubicin on tumor cells.

Moreover, its clinical efficacy is often limited by poor penetration into solid tumors, non-specific biodistribution, and a narrow therapeutic window.[6,7] Consequently, the development of novel therapeutic strategies that overcome these limitations without compromising the anticancer efficacy of doxorubicin is essential. To this end, a variety of nanosystems have been developed and evaluated as potential drug delivery platforms, including polymeric systems, cyclodextrin derivatives, dendrimers, liposomes, carbon nanostructures, mesoporous silicas, and metal nanoparticles, among others.[5,8] Compared to free drugs, numerous studies have demonstrated that drug delivery *via* these nanocarriers enhances drug bioavailability and cellular uptake of the drug, reduces toxicity to healthy tissues, and minimizes side effects.[9,10]

Among these nanosystems, nanoparticles offer distinct advantages such as passive tumor targeting through the enhanced permeability and retention (EPR) effect, high drug loading capacity, improved compound stability and solubility, and facilitated transport across cellular and tissue membranes,[11,12] making them particularly attractive. In particular, carbon dots (CDs) can provide additional benefits due to their intrinsic luminescent properties, ease of synthesis, and remarkable antioxidant activity, providing added value for therapeutic applications. As previously reported by our group,[13] functionalization of CDs with macromolecular structures such as cyclodextrins (Cyd) enables the development of nanoplatforms with high potential for drug delivery, owing to the host–guest complexation ability of cyclodextrins.[14] In addition, the versatility of carbon-based nanomaterials has been highlighted in recent years not only for drug delivery purposes but also for the treatment of complex diseases, including neurological disorders and brain tumors.[15] Likewise, advanced surface functionalization strategies, such as ligand or antibody conjugation, have been proposed as promising approaches to improve targeting specificity and broaden the therapeutic scope of nanocarrier-based systems.[16]

Although cyclodextrin-functionalized nanomaterials have been previously explored for drug delivery, systematic comparative studies on how cyclodextrin cavity size influences drug–carrier interactions in carbon dot-based systems remain limited. In particular, the effect of β- and γ-cyclodextrin functionalization on doxorubicin loading efficiency, release kinetics, and biological response has not been thoroughly investigated. Therefore, the novelty of the present work lies in the comparative evaluation of β- and γ-cyclodextrin-functionalized carbon dots as biocompatible nanocarriers for doxorubicin delivery, with special emphasis on how cyclodextrin cavity size modulates host–guest interactions and, consequently, nanocarrier performance. Furthermore, this work explores an ultrasound-assisted loading strategy as a rapid and operationally simple method for drug encapsulation, which may offer practical advantages for the preparation of these nanoplatforms.

In this context, we propose the use of carbon dots modified with carboxymethyl-β-cyclodextrins (CM-β-Cyd) and carboxymethyl-γ-cyclodextrins (CM-γ-Cyd) as potential doxorubicin carriers, with the aim of preserving anticancer efficacy at the target site while mitigating systemic toxicity and minimizing side effects on healthy tissues. To assess this approach, various spectrometric techniques were employed to evaluate drug-carrier interaction. Drug loading and release studies were conducted, along with *in vitro* assays using human dermal fibroblasts (HDF) and lung carcinoma cells (A549). A comparative discussion with previously reported carbon dot-based doxorubicin nanocarriers is also included in order to better contextualize the advantages and limitations of the developed platforms within the current state of the art. Although the results are promising, further studies are required to assess their *in vivo* performance, including their stability in biological media, biodistribution and pharmacokinetics, to facilitate clinical translation.

Experimental

Materials

L-Glutathione (reduced), citric acid, β-cyclodextrin (β-Cyd), γ-cyclodextrin (γ-Cyd), *N*-(3-dimethylaminopropyl)-*N*′-ethylcarbodiimide hydrochloride (EDC·HCl), potassium dihydrogen phosphate (KH_2PO_4), potassium hydrogen phthalate, triethylamine, bromoacetic acid, and doxorubicin hydrochloride European Pharmacopoeia Reference Standard (Doxo) were purchased from Sigma-Aldrich. 10× Dulbecco's phosphate buffered saline (10× DPBS) and *N*-hydroxysulfosuccinimide sodium salt (sulfo-NHS) were obtained from Thermo Fisher

Scientific. Sodium hydroxide (NaOH), hydrochloric acid (HCl), methanol (MeOH), and absolute ethanol (EtOH) were acquired from VWR, while sodium citrate and chloroform were supplied by Acros Organics, and maleic acid by Fluka. The CellTiter 96® Non-Radioactive Cell Proliferation Assay Kit (Promega) was used for cell proliferation assays. Deionized Milli-Q water (MQW) was used throughout all experimental procedures.

Instrumentation

UV-visible absorption spectra were recorded using a Cary 60 UV-Vis Spectrophotometer, while excitation and emission luminescence spectra were acquired with a Varian Cary Eclipse Spectrofluorometer, both from Agilent Technologies. Attenuated Total Reflectance Fourier-Transform Infrared Spectroscopy (ATR-FTIR) spectra were collected using a Varian 670-IR Spectrometer in the range of 600–4000 cm^{-1} with 32 scans per spectrum. Thermogravimetric analysis (TGA) and single differential thermal analysis (SDTA) were carried out using a TGA/SDTA851 thermogravimetric analyzer (Mettler-Toledo), coupled to a Thermostar GSD301T Pfeiffer-Vacuum Mass Spectrometer. Elemental analysis (C, H, N, S) was performed with a Vario EL Elemental analyzer, using helium as carrier gas. X-ray photoelectron spectroscopy (XPS) measurements were performed with a PHOIBOS hemispherical analyzer, with monochromatized Al Kα radiation (1486.74 eV). Morphological and structural characterization were conducted using a high resolution-transmission electron microscope (HR-TEM) JEOL-JEM 2100F and analyzed with ImageJ software. Cell cycle analysis was performed on a Cytomics FC500 Flow Cytometer (Beckman Coulter).

Synthesis and modification of carbon dots

Different types of carbon dots (with and without surface modifications) were synthesized following procedures previously established by our research group.[13,17] Briefly, unmodified carbon dots (UCDs) were synthesized from reduced L-glutathione and citric acid *via* a hydrothermal method.[17] Simultaneously, carboxymethyl-β- and γ-cyclodextrins (CM-β-Cyd and CM-γ-Cyd) were prepared through a reaction of β-Cyd and γ-Cyd with sodium hydroxide and bromoacetic acid in distilled water under controlled temperature and time conditions, followed by precipitation in pure methanol.[13] Finally, UCDs were functionalized with CM-β-Cyd or CM-γ-Cyd using sulfo-NHS/EDC·HCl activation protocol under nitrogen atmosphere. The resulting products were purified by liquid–liquid extraction, followed by dialysis. After freeze-drying, yellowish solids corresponding to β-Cyd-CD and γ-Cyd-CD were obtained.

For further purification, 20 mg of each sample were separately transferred into centrifuge tubes, and 10 mL of pure ethanol were added. The mixtures were shaken on an orbital shaker at room temperature for 18 hours in the dark. Subsequently, the tubes were centrifuged at 5300 rpm for 25 minutes, and the supernatants were discarded. A solid phase, corresponding to the modified CDs, was observed at the bottom of the tubes. The solids were vacuum-dried overnight. This purification step was repeated by adding another 10 mL of ethanol to the dried solids, shaking again for 18 hours, and centrifuging under the same conditions. The supernatants were collected for absorbance analysis, and the remaining solids were dried and stored for further use.

Evaluation of cyclodextrin–doxorubicin interaction

The interaction between doxorubicin and modified cyclodextrins was evaluated by UV-visible absorbance measurements. The concentration of doxorubicin was kept constant at 2×10^{-5} M, while the concentration of CM-β-Cyd or CM-γ-Cyd was varied from 0 to 1×10^{-2} M. Likewise, natural cyclodextrins (β-Cyd and γ-Cyd) were evaluated under the same conditions as control samples. Shifts in the position of absorption bands and/or changes in their intensity, as well as the appearance of new bands, were used as indicators of the formation (or absence) of inclusion complex between doxorubicin and the cyclodextrins under study.

Loading and controlled release of doxorubicin

Evaluation of loading capacity in ethanolic medium. Doxorubicin was loaded into the purified β-Cyd-CD and γ-Cyd-CD by incubating 3 mg of each solid with 6 mL of an ethanolic doxorubicin solution (2×10^{-4} M). The mixtures were shaken on an orbital shaker at room temperature for 18 hours in the dark. Subsequently, the tubes were centrifuged at 5300 rpm for 25 minutes, and the supernatants were collected. The amount of doxorubicin effectively loaded onto the nanoplatforms was determined by measuring the absorbance of the collected supernatants (spectra recorded in the 200–800 nm range). An external calibration curve was prepared using ethanolic doxorubicin solution at concentrations ranging from 1.3×10^{-5} to 3.9×10^{-5} M.

Ultrasound-assisted nanoplatforms loading. Initially, 6 mL of a 3.5×10^{-4} M aqueous doxorubicin solution was ultrasonicated for 30 seconds and subsequently filtered through a 0.45 μm pore size cellulose acetate syringe filter to prevent the formation of aggregates, which could interfere with the drug-loading process. Next, 3 mg of each type of CD (β-Cyd-CD and γ-Cyd-CD) were suspended into 3 mL of the filtered doxorubicin solution. The resulting mixtures were subjected to ultrasound for 3 minutes to promote drug loading into the nanoplatforms. Immediately after this step, the samples were dialyzed as described in Section 2.5.3. to evaluate their release kinetics profile.

Controlled release studies. Controlled release of doxorubicin from the nanoplatforms was evaluated using a dialysis-based method, adapted from the procedure described by Schwarzl *et al.*[18] Both loading methods described in Sections 2.5.1 and 2.5.2 were assessed. For ethanolic medium-loaded β-Cyd-CD and γ-Cyd-CD samples, 3 mg of each solid were dissolved in 3 mL of Milli-Q water. Afterwards, 2 mL of each solution were separately transferred into individual dialysis bags (MWCO: 3.5 kDa). For ultrasound-assisted loaded samples, 2 mL of each preparation were also transferred into individual dialysis bag immediately after preparation.

In all cases, the dialysis process was carried out against 90 mL of 1× PBS, under constant magnetic stirring and dark

conditions, in a temperature-controlled room maintained at 37 °C. Over a 7 hours period, 300 μL aliquots were periodically withdrawn from the external medium and replaced with an equal volume of fresh 1× PBS to maintain the volume constant. In the same manner, a control experiment was also performed by introducing 2 mL of an aqueous doxorubicin solution (3.5×10^{-4} M) into a dialysis bag, in the absence of any CD-based carrier.

***In vitro* studies.** *In vitro* studies were conducted on the following cell lines: human dermal fibroblasts (healthy cell line) and A549 cells (lung carcinoma). Both cell lines were seeded at a concentration of 5000 cells per well and were cultured in an incubator under controlled conditions (37 °C, 5% CO_2 atmosphere) in DMEM medium containing 10% heat-inactivated fetal bovine serum, supplemented with 100 U mL^{-1} penicillin and 50 mg mL^{-1} streptomycin. These are referred to as 'standard conditions' throughout this study.

Cytotoxicity assay. The cytotoxicity of the products was assessed using a cell proliferation assay, also known as MTT assay, over a four-day period. Both cell lines were exposed to the following: 0.05 and 0.50 mg mL^{-1} of β-Cyd-CD and γ-Cyd-CD without doxorubicin, 0.05 and 0.50 mg mL^{-1} of β-Cyd-CD and γ-Cyd-CD loaded with doxorubicin (equivalent to 1.10 and 11.0 μg Doxo mL^{-1} for β-Cyd-CD and 0.35 and 3.50 μg Doxo mL^{-1} for γ-Cyd-CD, based on the loading test results), and four corresponding concentrations of solutions containing only Doxo (0.35, 1.10, 3.50 and 11.0 μg Doxo mL^{-1}). As a control, 1× PBS was added to both cell lines, the same volume used for the nanoplatforms.

The cytotoxicity of all the aforementioned products was evaluated using a MTT assay over a four-day period on healthy and tumour cell lines, both cultured and kept under the 'standard conditions'. This assay is based on assessing the activity of the mitochondrial enzyme succinate dehydrogenase, which converts the yellow MTT salt into insoluble blue formazan crystals.[19] The absorbance of these crystals is measured at 570 nm, and cell viability (%) was calculated according to the following equation:[19]

$$\text{Cell viability } (\%) = \frac{A_{x,\text{h}}}{A_{0,\text{h}}} \times 100$$

where $A_{x,\text{h}}$ is the average absorbance of the sample at different time points, and $A_{0,\text{h}}$ is the average absorbance of the cells on the first day of the experiment.

Cell cycle evaluation. Cellular internalization of the materials was assessed by flow cytometry, using the following procedure. Firstly, cells from both cell lines (healthy and tumor) were seeded in 6-well plates and were brought into contact with 0.1 mg mL^{-1} and 0.25 mg mL^{-1} of β-Cyd-CD, with and without the loaded drug, for a 48 hour period under controlled conditions (37 °C and 5% CO_2). Parallel experiments were conducted using equivalent concentrations of free doxorubicin. As negative controls, cells were cultured in the absence of both nanomaterials and doxorubicin.

Following exposure of the cells, samples were prepared for cell cycle analysis by fluorescence-activated cell sorting (FACS).[20] Briefly, cells were washed with 1× PBS and detached from the well using 0.25% trypsin solution in 0.5 mM ethylenediaminetetraacetic acid (EDTA). Then, approximately 1×10^6 cells were collected from each line, which were subjected to a second wash with 1× PBS. After centrifugation (1200 rpm, 5 minutes), the supernatants were discarded, and cells were resuspended in 250 μL of 1× PBS. For flow cytometric assays, 5 μL of ribonuclease A (10 mg mL^{-1}) were added to the cells and allowed to react for 10 minutes. Finally, 10 μL of propidium iodide (1 mg mL^{-1}) were also added, and the samples were kept in the dark until FACS analysis was performed.

Results and discussion

Synthesis and morphological/structural characterization of carbon dots

Carbon dots (CDs) modified with cyclodextrins, β-Cyd-CD and γ-Cyd-CD, were successfully synthesized *via* a hydrothermal method, followed by a functionalization using carboxymethyl-β/γ-Cyd through EDC·HCl/sulfo-NHS activation, as previously reported.[13] The hydrothermal synthesis of carbon dots from citric acid and glutathione typically yields nanoparticles bearing abundant oxygen- and nitrogen-containing surface functional groups, including carboxyl (–COOH), hydroxyl (–OH), sulfhydryl (–SH) and amine ($–NH_2$) moieties. These functional groups play a crucial role in enabling further chemical modification of the carbon dot surface.

In the present work, covalent conjugation between carbon dots and carboxymethylated cyclodextrins occurs through carbodiimide-mediated coupling chemistry. In this process, the carboxyl groups of CM-β-Cyd or CM-γ-Cyd are first activated by EDC·HCl in the presence of sulfo-NHS, generating reactive NHS-esters. These activated intermediates subsequently react with the amine groups present on the surface of the carbon dots, resulting in the formation of stable amide bonds that anchor the cyclodextrin molecules onto the nanoparticle surface. This strategy allows the hydrophobic inner cavity of the cyclodextrins to remain accessible for host–guest complexation with doxorubicin molecules.

Since the primary objective was to employ these modified CDs as nanocarriers for doxorubicin (Doxo) delivery, it was essential to minimize the presence of unmodified CDs (UCDs) to ensure optimal drug loading and release properties.

To achieve this, a purification strategy based on the differential solubility of the CD was applied: UCDs are fully soluble in ethanol, whereas the modified β-Cyd-CD and γ-Cyd-CD are insoluble in this solvent, enabling their selective separation. This difference in solubility arises from the increased molecular size and reduced polarity of the cyclodextrin-functionalized nanostructures compared with the smaller unmodified carbon dots. Consequently, ethanol washing allows efficient removal of residual UCDs while retaining the functionalized nanoplatforms.

By exploiting this solubility contrast of UCD and Cyd-CD, a significant reduction in the presence of UCD in the derivatized

material was achieved, as confirmed by UV-Vis absorbance measurements (λ_{max} = 345 nm). The residual UCD content was negligible, with purities greater than 93% for β-Cyd-CD and over 99% for γ-Cyd-CD, confirming that both samples were sufficiently purified for subsequent drug loading and characterization.

ATR-FTIR analysis of carboxymethyl cyclodextrins revealed a prominent peak at 1595 cm^{-1}, confirming the successful incorporation of a carboxyl group into the cyclosaccharide structure.[21] Following conjugation with UCDs, C–O stretching bands associated with primary and secondary hydroxyl groups (1020 and 1076 cm^{-1}, respectively) were observed in β-Cyd-CD and γ-Cyd-CD samples, indicating successful surface functionalization of UCDs with carboxymethylated cyclodextrins. Additionally, the appearance and relative intensity of these bands suggest the presence of abundant hydroxyl functionalities associated with the cyclodextrin moieties grafted onto the carbon dot surface, further supporting the successful attachment of the macrocyclic structures.

Additionally, XPS analysis further supported the successful modification, showing the disappearance of the peak at 288.8 eV corresponding to higher oxidation states from carboxyl group binding. Elemental Analysis corroborated these findings, revealing an increased content of both carbon and hydrogen, as expected from the presence of cyclodextrins on CD surface. Together, these spectroscopic and elemental analysis results confirm the effective surface functionalization of the carbon dots with cyclodextrin units through covalent bonding.

The structural and morphological characterization of the developed UCDs, β-Cyd-CD and γ-Cyd-CD are, therefore, in agreement with previously reported data.[13] HR-TEM analysis revealed that both unmodified and modified CD exhibited a spherical morphology, with lattice spacings of approximately 0.24 nm, consistent with a graphitic structure, and diameters ranging from 3.0 to 3.6 nm.[20–22] Thermal stability was assessed *via* TGA and SDTA analysis, showing a characteristic three-step degradation pattern in all cases: (1) evaporation of adsorbed water molecules, (2) decomposition of oxygen- and nitrogen-containing surface groups, and (3) breakdown of the carbon core. The preservation of the nanoscale morphology after cyclodextrin functionalization indicates that the modification process does not significantly alter the structural integrity of the carbon dots, while introducing additional functional groups capable of interacting with drug molecules.

Spectroscopic characterization of the nanocarrier systems and doxorubicin

Vis-UV absorption spectra were recorded for doxorubicin and the nanocarrier systems under study. The profiles obtained in aqueous solution are shown in Fig. 2. The absorption spectrum of doxorubicin exhibits a characteristic band centered at 493 nm, attributed to π–π* electronic transitions.[23] β-Cyd-CD and γ-Cyd-CD displayed the typical absorption profile associated with carbon dots,[24] confirming that modification with CM-Cyd does not significantly alter their optical properties. In contrast, neither the native nor the modified cyclodextrins (β-Cyd, γ-Cyd, CM-β-Cyd and CM-γ-Cyd) displayed any significant UV-Vis absorption within the tested wavelength range.

Evaluation of cyclodextrin–doxorubicin interaction

The interaction between doxorubicin and the nanocarrier system was investigated by UV-Vis spectroscopy. The study initially focused on the interaction between doxorubicin with the modified cyclodextrins (CM-β-Cyd and CM-γ-Cyd) and was later extended to carbon dots functionalized with these cyclodextrins (β-Cyd-CD and γ-Cyd-CD). For all experiments, the concentration of doxorubicin was kept constant, while the concentration of CM-Cyd varied. Equivalent studies were also carried out with unmodified cyclodextrins, which served as control samples.

For simplicity, interaction studies were performed in aqueous solution, considering the pK_a values reported for these molecules.[23] At pH values above 6, CM-Cyd exists predominantly in its anionic form, while doxorubicin remains positively charged. Under these conditions, electrostatic attraction

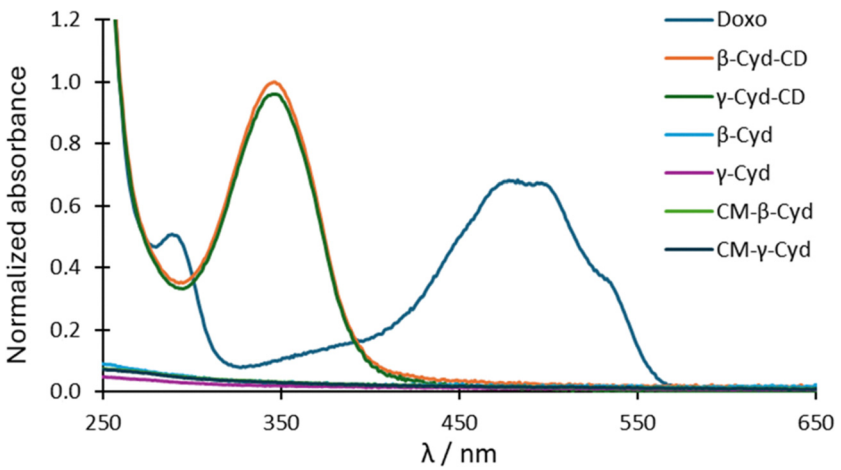

Fig. 2 Normalized absorption spectra of doxorubicin (2×10^{-5} M), β- and γ-Cyd (1×10^{-2} M), CM-β-Cyd and CM-γ-Cyd (1×10^{-2} M), and β- and γ-Cyd-CD (1 mg mL^{-1}) in aqueous solution.

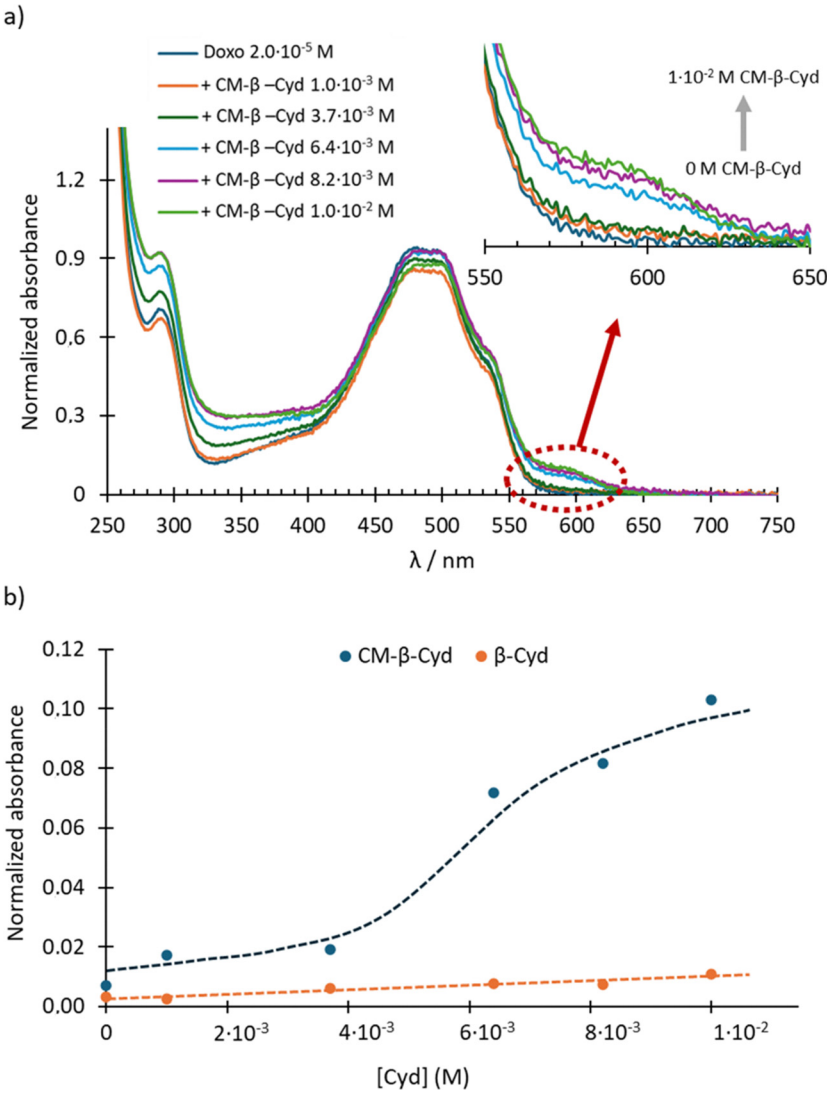

Fig. 3 (a) Normalized UV-Vis absorption spectra of doxorubicin (2×10^{-5} M) in the presence of different concentrations (0–1×10^{-2} M) of CM-β-Cyd, the inset highlights the progressive increase of the absorbance band at 592 nm associated with host–guest complex formation, and (b) absorbance at 592 nm plotted against CM-β-Cyd and β-Cyd concentrations. Normalized to the maximum absorbance of the doxorubicin standard.

between the negatively charged carboxyl groups of CM-Cyd and the protonated amino groups of doxorubicin may contribute to stabilizing the interaction between both species, in addition to the host–guest complexation occurring inside the cyclodextrin cavity.

Fig. 3a shows the UV-Vis absorption spectra of aqueous solutions of doxorubicin (2×10^{-5} M) in the presence of increasing concentrations of CM-β-Cyd ranging from 0 to 1×10^{-2} M. A new band centered at 592 nm appears upon the addition of CM-β-Cyd, which can be attributed to the formation of an inclusion complex. In contrast, no significant spectral changes were observed with unmodified β-Cyd (see Fig. 3b), suggesting that stable complexes do not occur, or form only to a much lesser extent, under the same conditions. These results for laboratory-synthesized CM-β-Cyd are consistent with previous reports describing the interaction of doxorubicin with commercial β-Cyd and CM-β-Cyd.[23]

Although the spectral changes observed in Fig. 3a are relatively subtle, the progressive increase in the absorbance at 592 nm with increasing CM-β-Cyd concentration indicates the formation of a weak but detectable interaction between doxorubicin and the modified cyclodextrin. This behavior is consistent with host–guest complexation equilibria involving relatively low binding constants, where the spectral variations may not show a strictly linear dose-dependent trend but still reflect the formation of inclusion complexes. This difference can be rationalized considering the internal cavity size of the cyclodextrins. β-Cyclodextrin possesses an internal cavity diameter of approximately 6–6.5 Å, which provides a suitable steric match for the aromatic rings of doxorubicin, favoring hydrophobic interactions and stabilizing the host–guest complex. In contrast, γ-cyclodextrin has a significantly larger cavity (~8 Å), which may reduce the strength of the interaction due to weaker molecular confinement of the drug inside the cavity.[25]

Additionally, the presence of carboxymethyl substituents on the modified cyclodextrins introduces negatively charged groups that may further stabilize the interaction with doxorubicin through electrostatic attraction. However, this effect appears to be more relevant in the case of CM-β-Cyd, where the geometric compatibility between the cyclodextrin cavity and the doxorubicin molecule favors the formation of a more stable supramolecular complex.

Therefore, the spectroscopic results suggest that the interaction between doxorubicin and the nanocarrier system is mainly governed by a combination of host–guest inclusion within the cyclodextrin cavity and electrostatic interactions between the drug and the functional groups present on the modified cyclodextrins.

Although the interaction observed for CM-γ-Cyd appears to be weaker or negligible under the conditions studied, these results provide useful insight into how cyclodextrin cavity size can influence drug–carrier interactions in carbon dot-based nanoplatforms.

Loading and controlled release of doxorubicin in solution

Two different methodologies were employed to load doxorubicin onto the nanoplatforms: (i) orbital shaking under mild conditions for an extended period in ethanolic medium, and (ii) ultrasound-assisted loading involving a short contact time in aqueous solution. In the first approach, a fixed amount of β-Cyd-CD (or γ-Cyd-CD) was mixed with an ethanolic solution of doxorubicin, and the mixtures were subjected to orbital shaking for 18 hours in the dark. In the ultrasound-assisted method, the CD-based nanoplatforms were combined with a filtered aqueous solution of doxorubicin and subjected to sonication for 3 minutes to promote drug loading. The use of two different loading strategies allowed evaluation of how the loading conditions influence the interaction between doxorubicin and the cyclodextrin-functionalized nanocarriers. In both cases, the dialysis process was initiated immediately after the loading step, as detailed in the following section.

Evaluation of loading capacity in ethanolic medium

The concentration of free (unloaded) doxorubicin in the supernatants, after loading by orbital shaking method, was quantified based on the absorbance measurements. From these data, the amount of drug present in the nanomaterials was calculated by difference with respect to the initial concentration. The results showed that 42.4% and 13.4% of the initial doxorubicin was effectively incorporated into β-Cyd-CD and γ-Cyd-CD, respectively. According to prior findings from our research group, the percentage of cyclodextrins in β-Cyd-CD and γ-Cyd-CD is 81% and taking into account that only a fraction of these moieties (approximately 1/6 for β-Cyd and 1/7 for γ-Cyd) are active and available to form inclusion complexes,[13] it is possible to estimate the proportion of cyclodextrins that successfully interacted with doxorubicin. Based on the retention data obtained, around 34% of the active β-Cyd moieties were effectively complexed with the drug, whereas in the case of γ-Cyd, the value was notably lower (14%).

This marked difference in loading efficiency can be attributed to the different cavity sizes of the cyclodextrins. The internal cavity of β-cyclodextrin provides a better steric match for the aromatic rings of doxorubicin, favoring host–guest complex formation and stabilizing the drug inside the cyclodextrin cavity. In contrast, the larger cavity of γ-cyclodextrin results in weaker confinement of the drug molecule, which likely reduces the stability of the inclusion complex and consequently decreases the loading efficiency.

These results support the hypothesis that the interaction between doxorubicin and the nanoplatforms is primarily governed by host–guest inclusion within the cyclodextrin cavity, complemented by secondary electrostatic interactions between the positively charged drug and the negatively charged functional groups present on the modified carbon dots.

Controlled release studies and kinetics evaluation

Dialysis is a widely employed technique to evaluate the release behavior of drug-loaded nanocarriers.[18] This procedure involves the use of a semi-permeable cellulose membrane to separate the nanocarrier from the external release medium, resulting in two sequential steps that must be considered independently: from the one side, the diffusion of the drug through the dialysis membrane and from the other, the release of the drug from the nanocarrier itself. To evaluate these contributions separately, two types of experiments were performed: dialysis of a free doxorubicin solution (in absence of nanocarriers) and dialysis of a solution of doxorubicin-loaded nanocarriers (either β-Cyd-CD or γ-Cyd-CD). Thus, the release process of doxorubicin release proceeds in two consecutive stages: (1) release of the drug from the modified CDs into the internal medium (inside the dialysis membrane), followed by (2) the transfer of the drug into the external solution by diffusion through the dialysis membrane.

Since these processes occur sequentially rather than simultaneously, the overall release behavior can be described by a series resistance model for mass transfer, in which both the release from the nanocarrier and the diffusion through the dialysis membrane contribute to the observed kinetics.[22]

Dialysis experiments were conducted over a 7 hour period under controlled conditions. Aliquots were withdrawn at predetermined intervals and subsequently analyzed spectrophotometrically. Fig. 4 shows the doxorubicin release profiles for ultrasound-loaded β-Cyd-CD and γ-Cyd-CD, along with the control (free doxorubicin).

Although the overall shape of the release curves appears similar for free doxorubicin and the nanocarrier systems, a closer analysis of the kinetic parameters reveals a clear difference in the release rate. In particular, the presence of cyclodextrin-functionalized carbon dots leads to a measurable reduction in the effective release constant compared with the free drug.

Equivalent studies were carried out with β-Cyd-CD and γ-Cyd-CD loaded using the ethanolic method, following the same dialysis procedure described in Section 2.5.3. Fig. 5 depicts the obtained profiles, showing the same trend as those loaded by ultrasound.

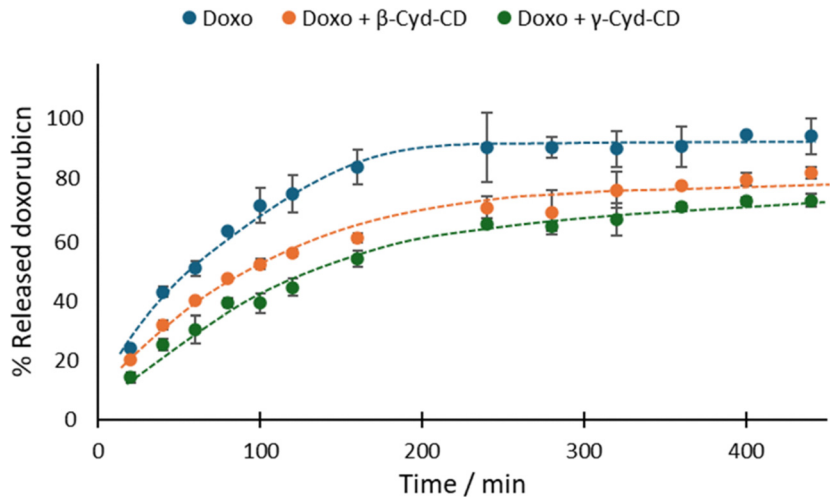

Fig. 4 Release profiles of doxorubicin through the dialysis membrane after ultrasound-assisted loading on β-Cyd-CD and γ-Cyd-CD, together with the doxorubicin control test.

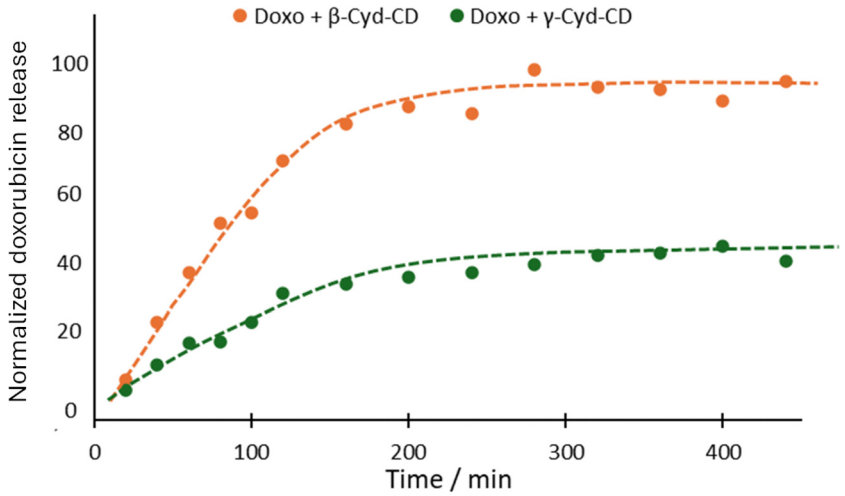

Fig. 5 Release profiles of doxorubicin through the dialysis membrane after loading on β-Cyd-CD and γ-Cyd-CD in ethanolic medium.

Importantly, the kinetic analysis indicates that the release rate of doxorubicin from the nanocarrier systems is significantly slower than that of free doxorubicin. Depending on the loading method and nanoplatform composition, the effective release rate was reduced by approximately 25–60% compared with the free drug.

This reduction in release rate suggests that the interaction between doxorubicin and the cyclodextrin-functionalized carbon dots introduces an additional barrier to drug diffusion, which can be attributed to the combined effects of host–guest inclusion within the cyclodextrin cavity and adsorption interactions at the carbon dot surface.

Therefore, even though the overall release profiles show similar qualitative behavior, the presence of the nanocarriers clearly modulates the release kinetics of doxorubicin, resulting in a slower and more controlled release process compared with free drug diffusion.

Such moderated release behavior may be advantageous for chemotherapy applications, as it may help maintain therapeutic drug concentrations over extended periods while avoiding the high peak concentrations typically associated with systemic toxicity.

Kinetics of doxorubicin through the dialysis membrane

To assess the impact of the dialysis membrane itself on the release process, various kinetic models were applied. Initially, the empirical Korsmeyer–Peppas model[26] was used to evaluate the dominant release mechanism, based on eqn (1):

$$\Phi_t = \kappa \cdot t^{\eta} \quad (1)$$

where Φ_t is the fraction of doxorubicin released at time t, κ is the release rate constant, and η is the diffusion coefficient. Φ_t values for each aliquot were calculated relative to the initial amount of doxorubicin inside the dialysis membrane (7×10^{-7} mol). Taking the logarithms of both sides, eqn (1) becomes the linear form shown in eqn (2):

$$\ln(\Phi_t) = \ln(\kappa) + \eta \ln(t) \quad (2)$$

Thus, by plotting $\ln(\Phi_t)$ *vs.* $\ln(t)$, the value of the diffusion coefficient (η) is obtained, corresponding to the slope of eqn (2). The value of η provides an insight into the underlying mechanism controlling the release of the drug through the dialysis membrane:[27] $\eta \sim 0.5$ indicates that the release is governed by Fickian diffusion, *i.e.* simple diffusion; if $0.5 < \eta < 1$, suggests that the mechanism is controlled by anomalous diffusion involving additional membrane effects, and finally, if $\eta > 1$, this points to complex release process involving several effects that occur simultaneously, such as membrane swelling at the same time as drug diffusion takes place.[24]

For comparative purposes and to evaluate the potential effect of β-Cyd-CD or γ-Cyd-CD on the doxorubicin release process, the same treatment was performed for the data obtained from both ultrasound-assisted loading method and CD loaded in ethanolic medium. Table 1 summarizes the regression statistics for all experimental values. The critical *F*-value (4.84) was calculated for 13 data points per curve ($d_f = 11$) and a significance level, α, of 0.05. κ values were derived from the value of the *y*-intercepts of the linearized model (eqn (2)).

The slope-values (η) for free doxorubicin and for doxorubicin loaded *via* ultrasound into β-Cyd-CD and γ-Cyd-CD were close to 0.5, indicating that the release of doxorubicin through the dialysis membrane follows Fickian diffusion, as well the diffusion of doxorubicin from both Cyd-CD systems. In these cases, solute release was primarily driven by the concentration gradient between the internal and external compartments,[28] consistent with the typical behavior of small-molecule diffusion through membranes.[24]

On the other hand, the free drug system (doxorubicin without Cyd-CD) showed the highest release kinetics ($\kappa_{free} = 3.0\ h^{-1/2}$), as it occurs by a simple diffusion mechanism, with the concentration gradient being the main driving force of the process, which is generally fast. Both ultrasound-assisted Cyd-CD systems then exhibited slower kinetics ($k_{\beta,UA} = 2.1\ h^{-1/2}$, $k_{\gamma,UA} = 1.3\ h^{-1/2}$, significantly different from k_{free} with $p < 0.05$) suggesting that the velocity is limited by the releasing of the doxorubicin from the nanoplatform, rather than by the diffusion of doxorubicin though the dialysis membrane. This agrees with the presence of an effective doxorubicin-nanoplatform interaction.

In contrast, the ethanolic-loaded β-Cyd-CD and γ-Cyd-CD systems exhibited poorer fits to the model, with lower correlation coefficients. In both cases η values exceeded 0.75, suggesting the predominance of anomalous diffusion and/or complex release processes involving multiple concurrent mechanisms.[27] Thus, the Korsmeyer–Peppas proposed model does not adequately describe release from nanocarriers loaded in ethanolic medium.

Release kinetics from nanocarriers

It has been described in the literature that the kinetics of drug release from nanocarriers can follow a first-order model,[29] expressed as eqn (3):

$$\Phi_t = 1 - \exp(-kt) \quad (3)$$

where Φ_t represents the fraction of doxorubicin released at each time (t) and κ is the release constant, expressed in units of time^{-1}. By taking the natural logarithm, eqn (3) can be easily converted into the linear eqn (4):

$$\ln(1 - \Phi_t) = -\kappa t \quad (4)$$

Table 2 presents the regression statistics obtained by fitting the experimental data according to eqn (4). The critical *F* value was calculated considering 13 data for the tests involving free doxorubicin and ultrasound-assisted loading while there were 9 data for the tests carried out with Cyd-CD loaded in ethanolic medium. The significance level, α, was set at 0.05.

Assuming a first-order release rate, similar to that used to describe the dissolution of aqueous-soluble compounds from porous matrices,[24] no statistically significant differences ($n = 13$, $p > 0.05$) were found between the release rates calculated for the ultrasound-assisted loaded materials. However, significant differences ($n = 9$, $p < 0.05$) were found between the two loading methodologies, particularly in the case of β-Cyd-CD loaded *via* the ethanolic method, whose value is 20% higher. These results suggest that doxorubicin loaded in ethanolic medium onto γ-Cyd-CD is released faster than in any other system. This is expectable when comparing γ-Cyd-CD and β-Cyd-CD loaded in ethanolic media, as γ-cyclodextrins have a weaker interaction with doxorubicin than β-cyclodextrins. Regarding the loading mechanism (ultrasound assisted *vs.* ethanolic medium), the additional energy supplied by the ultrasound may explain the more effective encapsulation of the drug and, therefore, a slower release rate.

In conclusion, the presence of nanocarriers reduces the release rate by 25–60% compared to free doxorubicin, regardless of the kinetic model applied. This fact may have positive implications for chemotherapy treatment, resulting in a more controlled and sustained drug release. Additionally, a slower release may help to minimize peaks in drug concentration in the body, potentially reducing the risk of acute toxicity in healthy tissues.

Table 1 Regression statistics for doxorubicin release according to Korsmeyer–Peppas model

System	$\ln(\kappa)$	κ	η	R	F
Doxo	-2.9 ± 0.2	$3.0 \pm 0.6\ h^{-1/2}$	0.43 ± 0.04	0.951	103.6
Doxo/β-Cyd-CD (ultrasound-assisted)	-3.3 ± 0.1	$2.1 \pm 0.36\ h^{-1/2}$	0.46 ± 0.03	0.976	218.4
Doxo/γ-Cyd-CD (ultrasound-assisted)	-3.8 ± 0.2	$1.32 \pm 0.24\ h^{-1/2}$	0.53 ± 0.04	0.973	192.9
Doxo/β-Cyd-CD (ethanolic medium)	-6 ± 1	$0.24 \pm 0.24\ h^{-1}$	1.1 ± 0.2	0.844	27.4
Doxo/γ-Cyd-CD (ethanolic medium)	-4.2 ± 0.4	$0.96 \pm 0.36\ h^{-0.74}$	0.74 ± 0.07	0.973	86.5

Table 2 Regression statistics for doxorubicin release from β-Cyd-CD and γ-Cyd-CD according to a first-order model

System	κ (day^{-1})	R	F	F_c
Doxo/β-Cyd-CD (ultrasound-assisted)	2.3 ± 0.1	0.951	114.8	4.75
Doxo/γ-Cyd-CD (ultrasound-assisted)	2.0 ± 0.1	0.948	106.5	4.75
Doxo/β-Cyd-CD (ethanolic medium)	19 ± 1	0.969	126.2	5.32
Doxo/γ-Cyd-CD (ethanolic medium)	2 ± 1	0.948	175.3	5.32

R values above 0.9 in all cases, together with F values exceeding the critical threshold, F_c, indicated a good fit to the proposed model.

In vitro studies

Proliferation assays. Cell proliferation studies were carried out using two cell lines, human dermal fibroblasts (HDF) and lung carcinoma cells (A549), over a 72 hours period. To this end, the mitochondrial activity was evaluated after exposing both cell lines to the two types of nanoplatforms, both loaded and unloaded with doxorubicin, at concentrations of 0.05 and 0.5 mg mL^{-1}. Based on the previously determined loading capacity, it is known that the concentration of doxorubicin loaded in 0.05 and 0.5 mg mL^{-1} of β-Cyd-CD is 1.1 and 11 mg mL^{-1}, respectively, whereas it is 0.35 and 3.5 μg mL^{-1} for γ-Cyd-CD, which had demonstrated a lower loading capacity. Solutions of free doxorubicin at the corresponding concentrations were also evaluated for comparison, together with untreated control cells.

Fig. 6 shows the results obtained for β-Cyd-CD. At a concentration of 0.05 mg mL^{-1} Cyd-CD alone behaved similarly to the control cells, proving that this concentration is not cytotoxic and therefore safe for use. However, when the concentration of these nanomaterials is 10 times higher, 0.5 mg mL^{-1}, a decrease in cell growth was observed.

When assessing the behavior of doxorubicin loaded β-Cyd-CD on HDF cell line (Fig. 6a) it was observed that at lowest concentration, cell growth was higher compared to free doxorubicin at the same concentration of 1.1 mg mL^{-1}, although the difference was not statistically significant. On the other side, at the highest concentration of loaded β-Cyd-CD, no differences were observed compared to free doxorubicin at 11 mg mL^{-1}. Results on line A549 show that the toxicity induced by the drug-loaded platforms in these cells is higher than in the healthy ones, especially at the highest concentrations, and they behaved almost identically to free doxorubicin (Fig. 6b). This could be explained by two factors: (1) the faster metabolism of tumor cells, and (2) the increased number of free radicals in tumor environments, which leads to CD being in their radical form.[30,31] In brief, drug loading on β-Cyd-CD seems to cause a lower toxic effect in cultured dermal fibroblasts than in lung carcinoma cells. Regarding the unloaded platforms, they showed potential to reduce the side effects on normal cells during treatment, while maintaining effectiveness in tumor cells.

The results obtained for γ-Cyd-CD are different from those obtained for β-Cyd-CD (see Fig. S1). Loaded nanoplatforms exhibit a cytotoxic effect intermediate between the unloaded platforms and free doxorubicin on both cell lines. Although γ-Cyd-CD did not show significant cytotoxic by themselves, their advantages for doxorubicin transport were less remarkable than those observed for β-Cyd-CD.

According to cell penetration studies previously reported by our group,[13] both β-Cyd-CD and γ-Cyd-CD are effectively internalized in both cell lines, maintaining their intrinsic fluorescent properties once inside the cells. This property, combined with effective drug loading and release, would allow not only disease treatment but also real-time monitoring of the drug distribution throughout the body.

Considering the increased load on β-Cyd-CD, these are chosen for further evaluation of the cell cycle, detailed in the following section. For such studies, intermediate concentrations were tested to prevent systemic toxicity. Therefore, new cell proliferation assays were performed with 0.1 and 0.25 mg mL^{-1} of β-Cyd-CD (2.2 and 5.5 mg mL^{-1} of loaded doxorubicin, respectively) and the corresponding control tests of free doxorubicin at the same concentrations.

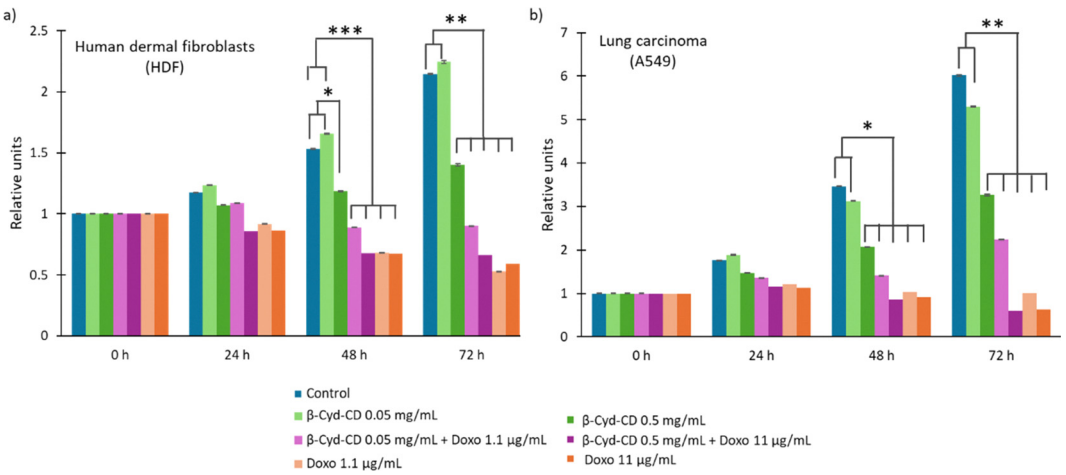

Fig. 6 Cell proliferation assays of β-Cyd-CD (0.05 and 0.5 mg mL^{-1}) loaded and unloaded with doxorubicin (1.1 and 11 mg mL^{-1}) on (a) HDF line and (b) A549 cell line. * Indicate the presence of significant differences (* $p < 0.05$, ** $p < 0.01$, *** $p < 0.005$).

Fig. S2a shows the results obtained on HDF line. As previously observed, β-Cyd-CD by themselves don't show any cytotoxic effect at the concentrations evaluated, presenting a similar behavior to that of the control cells up to 48 hours. After 72 hours, some growth inhibition was observed but it was not sufficient to compromise cell survival. Regarding doxorubicin-loaded CD, the induced cytotoxicity is similar to that of the free drug at the same concentration, with this trend being more evident after 48 hours of incubation in all cases.

When studying the A549 tumor line (Fig. S2b), it can be seen that β-Cyd-CD only caused some growth inhibition after 48 hours, although they were not inherently cytotoxic. Conversely, cell growth was significantly altered when exposed to both loaded β-Cyd-CD and free doxorubicin at the corresponding concentrations, particularly after 48 hours of incubation, as was also observed in the HDF cell line.

Overall, the results have demonstrated that the nanoplatforms themselves are well tolerated by both cell lines, with dermal fibroblasts showing especially high tolerance. This is particularly relevant for minimizing systemic toxicity during treatment. Furthermore, when the nanoparticles were loaded, the effects on both cell lines were comparable, with the antiproliferative effect characteristic of doxorubicin being maintained.

Cell cycle evaluation. The effect of β-Cyd-CD on the cell cycle was assessed employing the same concentrations as in the second cell proliferation assay, 0.1 and 0.25 mg mL^{-1} of β-Cyd-CD (2.2 and 5.5 mg mL^{-1} of loaded doxorubicin, respectively) along with free doxorubicin solutions. As shown in Fig. 7a, β-Cyd-CD alone did not significantly alter the cell cycle of HDF, being the proportion of cells in G1, S and G2 similar to the control ones. Nevertheless, a slight increase in G1 and a decrease in S were observed when using 0.25 mg mL^{-1} β-Cyd-CD, which may indicate inhibition of cell proliferation due to cytotoxic effects or cellular stress.[32]

Treatment with doxorubicin shows an antiproliferative effect, with an accumulation of cells in G1 phase whereas a G2 phase block was observed, leading to a reduction in the proportion of cells in S. This result is consistent with the known mechanism of action of doxorubicin which, as a chemotherapeutic agent, causes DNA damage and interferes with cell division.[5] The study of doxorubicin-loaded β-Cyd-CD revealed a greater impact on the cell cycle, notably with an increase proportion of cells in the G2 phase, suggesting a more pronounced block at the G2/M transition.

Similar studies carried out on line A549 (Fig. 7b) yielded comparable results. Unloaded β-Cyd-CD maintained a distribution similar to the control, while loaded with doxorubicin caused a decrease in the proportion of cells in G1 and an increase in G2, suggesting a blockage in the G2/M transition that prevented cells from completing mitosis. Lastly, treatment with doxorubicin shows similar behavior to that of the loaded β-Cyd-CD with an accumulation observed at the G2/M transition, suggesting a cytotoxic effect that blocks tumor cells in the late stages of the cell cycle.

It can be concluded that the presence of unloaded β-Cyd-CD did not cause significant alterations in the cell cycle of either cell lines, in agreement with the previously described proliferation results. In contrast, doxorubicin loading on nanoplatforms enhanced the cytotoxic effects of the drug, especially in the A549 tumor line, by promoting a strong block at the G2/M transition and preventing mitosis. These findings demonstrate that β-Cyd-CD used as drug carriers reinforce the antiproliferative effect of doxorubicin, while maintaining biocompatibility in healthy cells.

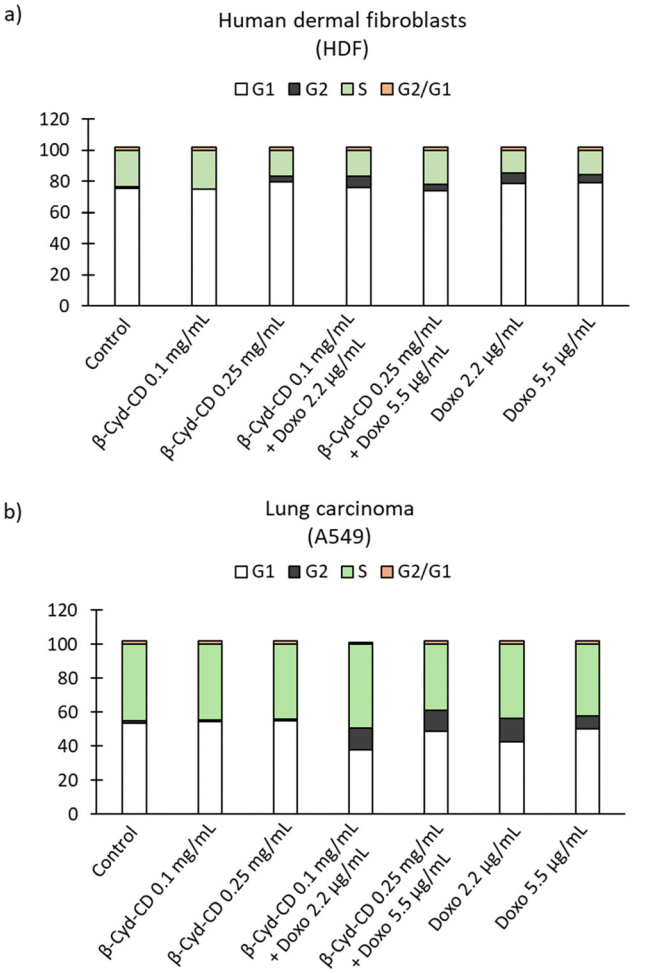

Fig. 7 Cell cycle of (a) HDF and (b) A549 line in contact with β-Cyd-CD (0.1 and 0.25 mg mL^{-1}), doxorubicin (2.2 and 5.5 mg mL^{-1}) and β-Cyd-CD loaded with doxorubicin.

Comparative discussion with previously reported carbon dot-based doxorubicin nanocarriers

To better contextualize the performance of the developed nanoplatforms, a comparison with representative carbon dot-based doxorubicin delivery systems reported in recent literature is summarized in Table 3. Recent studies confirm that carbon dots can be engineered to provide not only efficient drug loading, but also additional functionalities such as active targeting, pH-responsive release, enhanced cellular uptake, renal clearance, and combined theranostic performance. For instance, transferrin-conjugated carbon dots have been reported to improve targeted delivery of doxorubicin,[33] whereas folic acid-functionalized or

Table 3 Comparison of representative carbon dot-based nanocarriers for doxorubicin delivery reported in recent literature

System	Main design feature	Release/delivery behavior	Main reported advantage	Ref.
Transferrin-conjugated carbon dots (GCD-PEG-Tf@DOX)	PEGylated carbon dots functionalized with transferrin for receptor-mediated targeting	pH-responsive release with efficient uptake *via* transferrin receptor-mediated endocytosis	Enhanced tumor targeting and reduced toxicity toward normal cells	33
Folic acid carbon-dot nanoparticles (FA-CD-DOX)	Carbon dots functionalized with folic acid enabling receptor-targeted delivery	Drug release dependent on covalent *vs.* noncovalent DOX loading strategy	Improved therapeutic efficacy in folate-receptor-expressing cancer cells	34
Glucose-derived carbon dots–DOX system	CDs bearing aldehyde groups enabling acid-labile hydrazone conjugation with DOX	Acidic pH-responsive release triggered in tumor microenvironment	Enhanced cytotoxicity toward cervical cancer cells	35
Functional carbon dots (CT-CDs/DOX-CT-CDs)	Carbon dots synthesized by one-step pyrolysis enabling high drug loading	Biphasic release with sustained DOX release up to 144 h	High loading efficiency and good biocompatibility	36
Porphyrin-derived carbon dots (DOX@PCDs)	Porphyrin-based carbon dots enabling pH-responsive drug delivery and fluorescence imaging	Enhanced DOX release under acidic conditions typical of tumor microenvironments	Improved anticancer activity with reduced hemolysis and good biocompatibility	37
Renal-clearable sucrose carbon dots (Suc-CDs)	Ultra-small CDs enabling renal clearance and electrostatic DOX complexation	pH-dependent release with prolonged tumor accumulation	Reduced toxicity toward normal cells and improved therapeutic efficacy	38
Terbium-doped carbon dots (CD-Tb-DOX)	Rare-earth Tb-doped fluorescent CDs enabling theranostic drug conjugation	High adsorption (~92.5%) and controlled *in vitro* release (~89%)	Enhanced cytotoxicity against colon cancer cells and imaging capability	36
β-/γ-Cyclodextrin-functionalized carbon dots (β-Cyd-CD/γ-Cyd-CD)	Carbon dots covalently functionalized with carboxymethyl cyclodextrins enabling supramolecular host–guest DOX complexation	Moderated release kinetics (~25–60% slower than free DOX) governed by cyclodextrin inclusion	Comparative evaluation of β *vs.* γ cyclodextrin cavity size on drug loading and release	This work

glucose-derived carbon dot systems exploit ligand-assisted or acid-labile interactions to enhance intracellular delivery and pH-dependent release.[34] More recent studies have also described high-loading sustained-release carbon dots,[35,36] porphyrin-derived pH-responsive systems,[37] renal-clearable sucrose carbon dots,[38] and terbium-doped theranostic carbon dots for site-specific delivery.[39]

Within this context, the main contribution of the present work is not simply the use of carbon dots as doxorubicin carriers, but the comparative analysis of β- and γ-cyclodextrin-functionalized carbon dots as host–guest nanoplatforms. In particular, our study highlights how cyclodextrin cavity size influences drug–carrier interaction, loading efficiency, and release behavior. This supramolecular design feature differentiates the present system from many previously reported carbon dot carriers, which rely predominantly on electrostatic adsorption, covalent coupling, or ligand-mediated targeting. In addition, the ultrasound-assisted loading strategy explored here provides a rapid and operationally simple route for drug encapsulation, while the observed reduction in release rate relative to free doxorubicin supports the controlled-delivery character of the platform.

Conclusions

The interaction between β- and γ-cyclodextrin-functionalized carbon dots (Cyd-CDs) and the chemotherapeutic agent doxorubicin (DOX) was successfully confirmed by spectroscopic analyses, evidencing that the drug can be effectively loaded on these nanoplatforms through inclusion complex formation. Drug loading and release kinetics experiments revealed that both β-Cyd-CD and γ-Cyd-CD systems act as efficient nanocarriers, enabling high drug encapsulation efficiency and sustained release profiles, which may positively influence therapeutic performance.

Importantly, the comparative evaluation of β- and γ-cyclodextrin-functionalized carbon dots revealed that cyclodextrin cavity size plays a key role in modulating drug–carrier interactions. In particular, β-Cyd-CD exhibited significantly higher doxorubicin loading efficiency compared with γ-Cyd-CD, which can be attributed to the more favorable steric compatibility between the β-cyclodextrin cavity and the molecular structure of doxorubicin. These results highlight the relevance of supramolecular host–guest interactions as a design parameter in the development of carbon dot-based nanocarriers.

In vitro MTT assays demonstrated that DOX-loaded Cyd-CDs retained potent antiproliferative activity against tumor cells while exhibiting reduced cytotoxicity toward normal fibroblasts. Importantly, loading the nanoplatforms with doxorubicin did not compromise the drug's pharmacological activity. These results, supported by cell cycle analyses, indicate that Cyd-CD nanocarriers can maintain the anticancer efficacy of doxorubicin at targeted sites of action while potentially minimizing systemic toxicity.

Furthermore, kinetic analysis of the release experiments demonstrated that the presence of the cyclodextrin-functionalized nanoplatforms reduces the effective release rate of doxorubicin by approximately 25–60% compared with the free drug. This reduction indicates that host–guest inclusion within the cyclodextrin cavity introduces an additional resistance to drug diffusion, resulting in a moderated and more controlled release process. Such behavior may be advantageous for

chemotherapy applications, as it may help maintain therapeutic concentrations while avoiding the high peak drug levels associated with systemic toxicity.

Notable differences between β-Cyd-CD and γ-Cyd-CD highlight the critical role of cavity size and host–guest molecular architecture in modulating drug–carrier interactions, underscoring the importance of cyclodextrin selection in optimizing nanocarrier performance. Furthermore, the ultrasound-assisted loading approach proved to be a simple, rapid, and scalable strategy for drug encapsulation, offering advantages in terms of practicality and potential for future pharmaceutical applications.

Overall, the results presented here demonstrate that cyclodextrin-functionalized carbon dots represent a versatile supramolecular platform for anticancer drug delivery, combining the optical properties of carbon dots with the molecular recognition capability of cyclodextrins. In particular, the comparative analysis performed in this work provides valuable insight into how cyclodextrin cavity size influences drug loading and release behavior in carbon dot-based systems.

Although the results obtained are highly promising and open new avenues in cancer nanotherapy, their actual incorporation into clinical settings still requires additional studies to evaluate their *in vivo* behavior, including stability in biological media, biodistribution, and pharmacokinetics. A deeper understanding of these parameters will be essential to advance the rational design of Cyd-CD-based doxorubicin delivery systems and to translate these findings into safer and more effective nanomedicine-based cancer therapies.

Author contributions

SRV and TF: investigation, methodology and writing – original draft; JEC: methodology; AFG: conceptualization, formal analysis, visualization and writing – review and editing; SC: validation and writing – review and editing; RBL: conceptualization, supervision, funding acquisition, project administration.

Conflicts of interest

There are no conflicts to declare.

Data availability

The data supporting this article have been included as part of the supplementary information (SI). See DOI: https://doi.org/10.1039/d5tb02774h.

Acknowledgements

We gratefully acknowledge the support provided the University of Oviedo for its financial support through the project PAPI-24-GR-RECOMOL. Sandra Rodríguez Varillas was financially supported by The Principality of Asturias Administration under the Program Severo Ochoa for the research and education formation in the Principality of Asturias (grant number PA-21-PF-BP20-123).

References

1 S. A. Helmy, S. El-Mofty, A. M. El Gayar, I. M. El-Sherbiny and Y. M. El-Far, Novel doxorubicin/folate-targeted *trans*-ferulic acid-loaded PLGA nanoparticles combination: *in vivo* superiority over standard chemotherapeutic regimen for breast cancer treatment, *Biomed. Pharmacother.*, 2022, **145**, 112376, DOI: 10.1016/j.biopha.2021.112376.

2 M. F. Naief, S. N. Mohammed and A. M. Mohammed, Carbon nanotubes: a review on synthesis and drug delivery for cancer treatment, *Inorg. Chem. Commun.*, 2024, **159**, 111694, DOI: 10.1016/j.inoche.2023.111694.

3 L. Tang, J. Li, Q. Zhao, T. Pan, H. Zhong and W. Wang, Advanced and Innovative Nano-Systems for Anticancer Targeted Drug Delivery, *Pharmaceutics*, 2021, **13**(8), 1151, DOI: 10.3390/pharmaceutics13081151.

4 A. A. Sultan, G. A. Saad and G. M. El Maghraby, Permeation enhancers loaded bilosomes for improved intestinal absorption and cytotoxic activity of doxorubicin, *Int. J. Pharm.*, 2023, **630**, 122427, DOI: 10.1016/j.ijpharm.2022.122427.

5 H.-J. Kim, D.-G. Jeung and J.-M. Oh, Boosting the anticancer activity of doxorubicin with a layered double hydroxide nanocarrier, *Appl. Clay Sci.*, 2021, **203**, 106000, DOI: 10.1016/j.clay.2021.106000.

6 F. A. Boratto, *et al.*, Alpha-tocopheryl succinate improves encapsulation, pH-sensitivity, antitumor activity and reduces toxicity of doxorubicin-loaded liposomes, *Eur. J. Pharm. Sci.*, 2020, **144**, 105205, DOI: 10.1016/j.ejps.2019.105205.

7 M. A. Abd El-Salam, G. S. El-Tanbouly, J. K. Bastos and H. A. Metwaly, Novel antitumor activity of the combined treatment of galloylquinic acid compounds with doxorubicin in solid Ehrlich carcinoma model *via* the Notch signaling pathway modulation, *Life Sci.*, 2022, **299**, 120497, DOI: 10.1016/j.lfs.2022.120497.

8 S. G. Klochkov, *et al.*, Implications of nanotechnology for the treatment of cancer: recent advances, *Semin. Cancer Biol.*, 2021, **69**, 190–199, DOI: 10.1016/j.semcancer.2019.08.028.

9 F. ud Din, *et al.*, Effective use of nanocarriers as drug delivery systems for the treatment of selected tumors, *Int. J. Nanomed.*, 2017, **12**, 7291–7309, DOI: 10.2147/IJN.S146315.

10 H. Tonbul, *et al.*, Folic acid decoration of mesoporous silica nanoparticles to increase cellular uptake and cytotoxic activity of doxorubicin in human breast cancer cells, *J. Drug Delivery Sci. Technol.*, 2021, **63**, 102535, DOI: 10.1016/j.jddst.2021.102535.

11 Z. Zhang, *et al.*, Biomimetic carrier-free nanoparticle delivers digoxin and doxorubicin to exhibit synergetic antitumor activity *in vitro* and *in vivo*, *Chem. Eng. J.*, 2021, **406**, 126801, DOI: 10.1016/j.cej.2020.126801.

12 M. J. Mitchell, M. M. Billingsley, R. M. Haley, M. E. Wechsler, N. A. Peppas and R. Langer, Engineering precision

nanoparticles for drug delivery, *Nat. Rev. Drug Discovery*, 2021, **20**(2), 101–124, DOI: 10.1038/s41573-020-0090-8.

13 S. Rodríguez-Varillas, T. Fontanil, J. Espina Casado, A. Fernández-González and R. Badía Laíño, Surface modification of carbon dots with cyclodextrins as potential biocompatible photoluminescent delivery/bioimaging nanoplatform, *Anal. Chim. Acta*, 2024, **1318**, 342948, DOI: 10.1016/j.aca.2024.342948.

14 L. Ferreira, *et al.*, Cyclodextrin-based dermatological formulations: dermopharmaceutical and cosmetic applications, *Colloids Surf., B*, 2023, **221**, 113012, DOI: 10.1016/j.colsurfb.2022.113012.

15 D. Elsori, *et al.*, Nanotube breakthroughs: unveiling the potential of carbon nanotubes as a dual therapeutic arsenal for Alzheimer's disease and brain tumors, *Front. Oncol.*, 2023, **13**, 1265347, DOI: 10.3389/fonc.2023.1265347.

16 N. W. Nabih, *et al.*, Antibody-functionalized lipid nanocarriers for RNA-based cancer gene therapy: advances and challenges in targeted delivery, *Nanoscale Adv.*, 2025, **7**, 5905–5931, DOI: 10.1039/D5NA00323G.

17 T. Díaz-Faes López, A. Fernández González, M. E. Díaz-García and R. Badía-Laíño, Highly efficient Förster resonance energy transfer between carbon nanoparticles and europium–tetracycline complex, *Carbon*, 2015, **94**, 142–151, DOI: 10.1016/j.carbon.2015.06.066.

18 R. Schwarzl, F. Du, R. Haag and R. R. Netz, General method for the quantification of drug loading and release kinetics of nanocarriers, *Eur. J. Pharm. Biopharm.*, 2017, **116**, 131–137, DOI: 10.1016/j.ejpb.2016.12.015.

19 N. Rani, *et al.*, *In vitro* study of green synthesized ZnO nanoparticles on human lung cancer cell lines, *Mater. Today Proc.*, 2022, **49**, 1436–1442, DOI: 10.1016/j.matpr.2021.07.203.

20 M. J. Wilkerson, Principles and applications of flow cytometry and cell sorting in companion animal medicine, *Vet. Clin. North Am.: Small Anim. Pract.*, 2012, **42**(1), 53–71, DOI: 10.1016/j.cvsm.2011.09.012.

21 G. Socrates, *Infrared and Raman characteristic group frequencies: Tables and charts*, 3rd edn, 2001.

22 S. Bayda, E. Amadio, S. Cailotto, Y. Frión-Herrera, A. Perosa and F. Rizzolio, Carbon dots for cancer nanomedicine: a bright future, *Nanoscale Adv.*, 2021, **3**(18), 5183–5221, DOI: 10.1039/D1NA00036E.

23 T. Carmona, C. Fernández-Clavero, G. Marcelo and F. Mendicuti, Encapsulation of doxorubicin in carboxymethyl-β-cyclodextrin in aqueous medium mediated by pH-modulated electrostatics interactions, *J. Mol. Liq.*, 2023, **376**, 121512, DOI: 10.1016/j.molliq.2023.121512.

24 V. A. Chhabra, R. Kaur, N. Kumar, A. Deep, C. Rajesh and K.-H. Kim, Synthesis and spectroscopic studies of functionalized graphene quantum dots with diverse fluorescence characteristics, *RSC Adv.*, 2018, **8**(21), 11446–11454, DOI: 10.1039/C8RA01148F.

25 T. Kovacs, Nagy, G. Panyi, L. Szente, Z. Varga and F. Zakany, Cyclodextrins: only pharmaceutical excipients or full-fledged drug candidates?, *Pharmaceutics*, 2022, **14**(12), 2559, DOI: 10.3390/pharmaceutics14122559.

26 R. W. Korsmeyer, R. Gurny, E. Doelker, P. Buri and N. A. Peppas, Mechanisms of solute release from porous hydrophilic polymers, *Int. J. Pharm.*, 1983, **15**(1), 25–35, DOI: 10.1016/0378-5173(83)90064-9.

27 S. Cascone, Modeling and comparison of release profiles:effect of the dissolution method, *Eur. J. Pharm. Sci.*, 2017, **106**, 352–361, DOI: 10.1016/j.ejps.2017.06.021.

28 D. R. Paul, Elaborations on the Higuchi model for drug delivery, *Int. J. Pharm.*, 2011, **418**(1), 13–17, DOI: 10.1016/j.ijpharm.2010.10.037.

29 S. Rochín-Wong, *et al.*, Drug release properties of diflunisal from layer-by-layer self-assembled κ-Carrageenan/chitosan nanocapsules: effect of deposited layers, *Polymers*, 2018, **10**(7), 760, DOI: 10.3390/polym10070760.

30 S. Rodríguez-Varillas, T. Fontanil, Á. J. Obaya, A. Fernández-González, C. Murru and R. Badía-Laíño, Biocompatibility and antioxidant capabilities of carbon dots obtained from tomato (*Solanum lycopersicum*), *Appl. Sci.*, 2022, **12**(2), 773, DOI: 10.3390/app12020773.

31 V. Helfinger and K. Schröder, Redox control in cancer development and progression, *Mol. Aspects Med.*, 2018, **63**, 88–98, DOI: 10.1016/j.mam.2018.02.003.

32 N. Kumar and N. Borth, Flow-cytometry and cell sorting: an efficient approach to investigate productivity and cell physiology in mammalian cell factories, *Methods*, 2012, **56**(3), 366–374, DOI: 10.1016/j.ymeth.2012.03.004.

33 L. Li, Q. Zhang, J. Li, Y. Tian, Y. Kang, G. Ren, W. Liu and H. Wang, Targeted delivery of doxorubicin using transferrin-conjugated carbon dots for cancer therapy, *ACS Appl. Bio Mater.*, 2021, **4**, 7280–7289, DOI: 10.1021/acsabm.1c00811.

34 S. N. Dada, G. K. Babanyinah and M. T. Tetteh, *et al.*, Covalent and noncovalent loading of doxorubicin by folic acid-carbon dot nanoparticles for cancer theranostics, *ACS Omega*, 2022, **7**, 23322–23331, DOI: 10.1021/acsomega.2c01482.

35 N. Dubey, S. Ramteke, N. K. Jain, T. Dutta and A. L. Koner, Glucose-derived carbon dots for targeted delivery of doxorubicin in cancer therapy, *New J. Chem.*, 2023, **47**, 16390–16398, DOI: 10.1039/D3NJ02843G.

36 A. Prasad, R. P. Sekar and M. C. A. Razana, *et al.*, High loading and sustained-release system of doxorubicin-carbon dots as nanocarriers for cancer therapeutics, *Biomed. Mater.*, 2024, **19**(6), 065018, DOI: 10.1088/1748-605X/ad7f3a.

37 A. Ansary, A. Osman and M. E. El-Khouly, Doxorubicin-loaded pH-responsive porphyrin-derived carbon dots as a promising biocompatible drug delivery system for effective chemotherapy of breast cancer, *RSC Adv.*, 2025, **15**, 6457–6473, DOI: 10.1039/D4RA09058F.

38 F. Azmi, X. Xu and H. Duong, *et al.*, Renal clearable sucrose carbon dots for doxorubicin delivery to treat renal carcinoma, *Nanoscale Adv.*, 2025, **7**, 2751–2760, DOI: 10.1039/D4NA01082E.

39 D. Kalyanasundaram, P. M. Arockia Sagayaraj and T. Dasgupta, *et al.*, Doxorubicin-conjugated terbium-doped carbon dots for site-specific colon cancer theranostics, *ACS Appl. Nano Mater.*, 2025, **8**, 6274–6287, DOI: 10.1021/acsanm.4c06365.

